Inorganic Chemistry Communications 122 (2020) 108292

Contents lists available at ScienceDirect

Inorganic Chemistry Communications

journal homepage: www.elsevier.com/locate/inoche

One-pot liquid microwave-assisted green synthesis of neutral *trans*-$Cl_2Cu(NNOH)_2$: XRD/HSA-interactions, antifungal and antibacterial evaluations

Abderrahim Titi [a,*], Ismail Warad [b,*], Saud M. Almutairi [c], Mohammed Fettouhi [d], Mouslim Messali [e], Ateyatallah Aljuhani [e], Rachid Touzani [a], Abdelkader Zarrouk [f]

[a] Laboratory of Applied and Environmental Chemistry (LCAE), Mohammed first University, Oujda, Morocco
[b] Department of Chemistry and Earth Sciences, PO Box 2713, Qatar University, Doha, Qatar
[c] King Abdul-Aziz City for Science and Technology, Riyadh 11442, P.O. Box 6086, Saudi Arabia
[d] Department of Chemistry, King Fahd University of Petroleum and Minerals, P.O. Box 5048, Dhahran 31261, Saudi Arabia
[e] Department of Chemistry, Taibah University, 30002 Al-Madina Al-Mounawara, Saudi Arabia
[f] Laboratory of Materials, Nanotechnology and Environment, Mohammed V University, Faculty of Sciences, 4Av. Ibn Battuta, PO B.P. 1014, Rabat, Morocco

ARTICLE INFO

Keywords:
XRD
Cu(II) complex
Pyrazole
Biological activities

ABSTRACT

In the present work, the ethyl-1-(hydroxymethyl)-5-methy-3-carboxylatel pyrazole)NNOH(polydentate ligand was used to synthesize a new *trans*-$Cl_2Cu(NNOH)_2$ complex *via* one-port microwave short procedure using water medium with no side products. The complex composition was analyzed based on FT-IR, UV–Vis, CHN-EA and EDX. Its crystal structure was determined by single crystal X-ray diffraction analysis. Hirshfeld surface analysis (HSA) and two-dimension figure-print (2D-FP) for the complex have been performed. The antibacterial activities were investigated using four types of gram-negative and gram-positive bacteria. Furthermore, the antifungal activities were evaluated using four types of fungi.

1. Introduction

Pyrazole ligand and its derivatives represent an important class of O, N-polydentate organic compounds in chemistry and biology [1–4]. Such compounds have shown significant pharmacological and biological roles through activities such as antimalarial, antibacterial, antitumor, and anti-inflammatory [1–3]. For example, Pyrazole-positioning compounds comprise a part of the several available pharmaceutical medicines like PNU-32945, Doramapimod, and Celecobix [4–6]. The pyrazole derivative compounds are also used as analytical reagents, metal ions extractors, fabrication materials, switches/sensors molecules, optical memory cells and in field of selective catalysis [7–16].

There is a growing interest in chelating pyrazole ligands containing O, N and P atom donors, since several adjusted organic substituents can be attached to the pyrazoles backbone to enhance their chelating and biological properties [17–19]. The structural characterization of their metal complexes revealed a rich variety in their coordination geometries [19].

Herein, in this report, the *trans*-$Cl_2Cu(NNOH)_2$ complex has been prepared in one-pot aqua-green synthesis *via* MW radiation. The desired complex was spectrally characterized; the N∩O-chelating quality of the NNOH ligand and the structure of the complex has been determined by XRD. Moreover, the Hirshfeld surface analysis (HSA) and two-dimension figure-print (2D-FP) have been stimulated. The antifungal and antibacterial activities conducted for the complex have been evaluated against several types of fungi and bacterial families.

2. Experimental

2.1. Materials

The compound NNOH was synthesized by the condensation reaction of ethyl 5-methyl-3-carboxylate pyrazole, and paraformaldehyde and used after crystallization from the ethanol solvent. A CEM Discovery controllable single-mode microwave reactor with 2×10^6 Pa pressure and 300 W power condition was used [20]. While the IR spectra were recorded using a Perkin Elmer FT- IR spectrometer in the 4000–400 cm^{-1} range, the EDX was performed on JSM-6360 ASEM and UV–Vis. on TU-1901 double-beam UV–Vis spectrophotometer. The HSA was performed using the Crystal Explorer 3.1 program [21].

* Corresponding authors.
E-mail addresses: titi_abderrahim1718@upm.ac.ma (A. Titi), Ismail.warad@qu.edu.qa (I. Warad).

https://doi.org/10.1016/j.inoche.2020.108292
Received 16 September 2020; Received in revised form 5 October 2020; Accepted 5 October 2020
Available online 15 October 2020

Table 1
Refinement data of the desired crystal.

Empirical formula	$C_{16}H_{24}Cl_2CuN_4O_6$
CCDC	1,997,623
Formula weight	502.83
Temperature (K)	298(2)
Wavelength (Å)	0.71073
Crystal system Space group	Monoclinic, P $2_1/c$
a, b, and c (Å)	7.5981 (7), 12.9762 (12), and 11.7009 (11)
B(°)	107.790 (3)
Volume ($Å^3$), Z	1098.48 (18), 2
Density (g/cm^3) (calculated)	1.520
Absorption coefficient (mm^{-1})	1.276
F(0 0 0)	518
Theta range for data collection	3.140 to 28.385°
Index ranges	$-10 \le h \le 10$, $-17 \le k \le 17$, $-15 \le l \le 15$
Reflections collected	46,847
Independent reflections	2750 [R(int) = 0.0587]
Refinement method	Full-matrix least-squares on F^2
Data / restraints / parameters	2750 / 2 / 135
Goodness-of-fit on F^2	1.173
Final R indices [I > 2sigma(I)]	$R_1 = 0.0802$, $wR_2 = 0.1787$
R indices (all data)	$R_1 = 0.1147$, $wR_2 = 0.2050$
Largest diff. peak and hole ($e.Å^{-3}$)	1.560 and −0.962

2.2. Trans-Cl2Cu(NNOH)2 synthesis

Our protocol for the syntheses of *trans*-Cl2Cu(NNOH)2 has been performed under microwave irradiation condition. To the solution of 1.0 eq of NNOH in 40 ml of distilled water, solid 0.5 eq of CuCl2·.6H2O was added. The mixture was immediately transferred to an MW closed vessel that was subjected to Microwave irradiation for 2 min. To remove any unexpected solid impurities from the green complex solution, the mixture was filtered then left for evaporation at RT. After one day, green crystals of the complex were obtained with 82% yields. The IR main bands of the desired complex are listed as $\nu = 3425$ (O—H), 3050 ($C_{pyrazole}$—H), 2925 (C_{Me}—H), 1750 (C═O), 1610 (C═N), 1460 (C═C), 1355 (N═N), 1020 (C—O), 460 (Cu—O) and 445 cm^{-1} (Cu—N) respectively.

2.2.1. In vitro antibacterial and antifungal

The complex was screened in vitro for their antibacterial activity against two Gram-positive [*Bacillus subtilis (RCMB 015 1 NRRL B-543), Staphylococcus aureus* (*RCMB010010*)], and two Gram-negative [*Proteus vulgaris (RCMB 004 (1) ATCC 13315, Escherichia coli (RCMB 010052) ATCC 25955)]* bacterial strains *via* the agar-well diffusion method using stranded Gentamycin famous antibiotic. The detail antibacterial producer together with the other international antibacterial protocols have been used following recent literature [3].

Antifungal activities of the complex were studied, against four fungi strains [*Candida albicans* (*RCMB 005003 1 ATCC 10231*), A*spergillus flavus* (*RCMB 002002*), *Penicillium marneffeii,* and *Cryptococcus neoformas* (RCMB 0049001)]. Sabouraud dextrose agar was seeded with 105 (cfu) mL^{-1} fungal spore suspensions and transferred to petri plates. The reference used was Ketoconazole antifungal drug. The detailed international antifungal procedures and protocols have been performed according to literature [3].

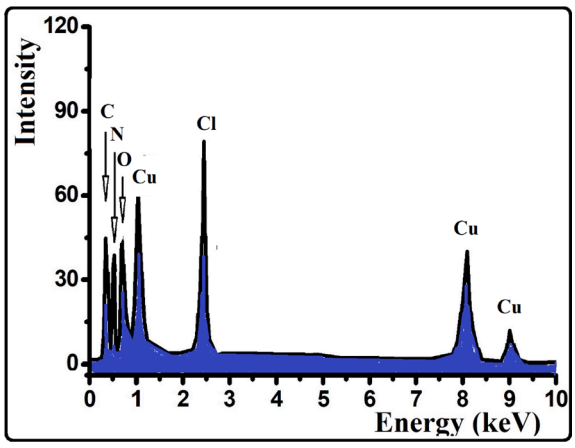

Fig.1. EDX spectra of the desired cluster.

2.3. XRD-Structure

The single crystal X-ray data of the complex were collected on a Bruker D8 Quest diffractometer (Mo-Kα radiation λ = 0.71073 Å). Data were recorded and integrated using Bruker APEX3 software package [22]. Multi-scan absorption correction was performed using SADABS [23]. The structure was solved by direct methods using SHELXS and SHELXTL package, refined using full-matrix least squares procedures on F^2 via the program SHELXL-2014 [24]. ORTEP3 was served for molecular graphics [25]. All hydrogen atoms were included at calculated positions using a-riding model with C—H distances of 0.93 Å for sp^2 carbons and 0.96–0.97 Å for sp^3 carbons. The isotropic displacement parameters were $U_{iso}(H) = 1.2U_{eq}(C)$ for methylene groups and sp^2 carbons and $U_{iso}(H) = 1.5U_{eq}(C)$ for methyl groups. The crystal data and refinement details are given in Table 1.

3. Results and discussion

3.1. Preparation, EDX, and CHN-elemental analysis

Under the mode of MW radiation, the desired complex has been synthesized in a very short time and without having side production cluster formation. An eco-friendly approach has been taken to prepare the desired complex in a one-pot reaction. In a minimum, a small amount of ethanol solvent two equivalent of NNOH was mixed with one equivalent amount of $CuCl_2{\cdot}6H_2O$ the reaction was subjected to MW for 2 min. (Scheme 1). In the first minute the mixture color turned to green, indicating a significant progress in the reaction, the desired complex, as a green powder, was collected in 82% yield. The classical approach without MW may require one-day stirring or 5 h reflux [8].

The desired complex was completely analyzed by several tools like FT-IR, UV–Vis, in addition, the 3D structure was solved by XRD-analysis, and the structure was subjected to HSA analysis to prove the interaction one surface of the complex. The CHN-Elemental analysis of the complex

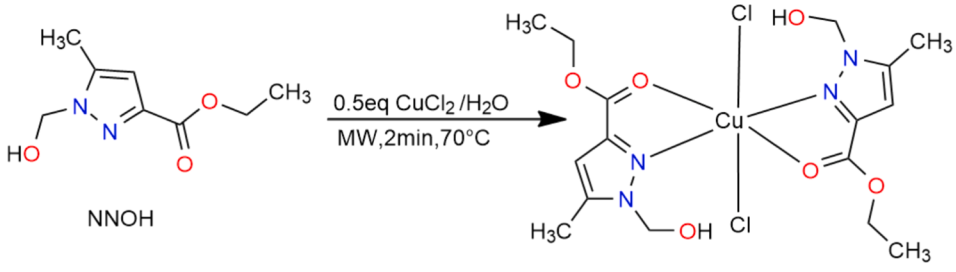

Scheme 1. Synthesis of the complex.

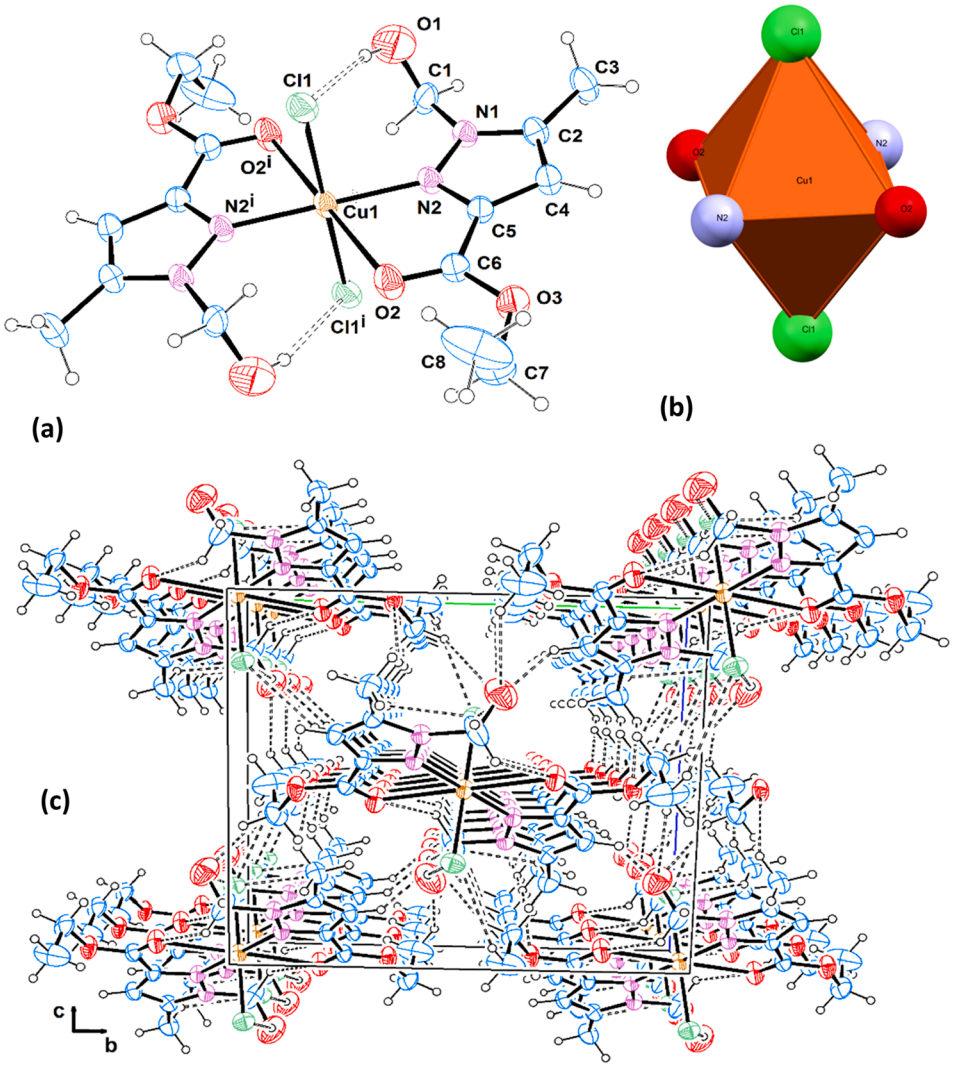

Fig. 2. Complex XRD-data (a) Molecular structure of the compound, (b) Distorted octahedral geometry and (c) Molecular packing including cell unit.

Table 2
Chosen angles [°] and bond lengths [Å].

No.	Bonds		Å	No.	Angles			[°]
1	Cu1	Cl1	2.283	1	Cl1	Cu1	N2	89.6
2	Cu1	N2	1.987	2	Cl1	Cu1	O2	93.9
3	Cu1	O2	2.565	3	Cl1	Cu1	Cl1	180
4	Cu1	Cl1	2.283	4	Cl1	Cu1	N2	90.4
5	Cu1	N2	1.987	5	Cl1	Cu1	O2	86.1
6	Cu1	O2	2.565	6	N2	Cu1	O2	72.4
7	N1	N2	1.344	7	N2	Cu1	Cl1	90.4
8	N1	C1	1.52	8	N2	Cu1	N2	180
9	N1	C2	1.351	9	N2	Cu1	O2	107.6
10	N2	C5	1.326	10	O2	Cu1	Cl1	86.1
11	O1	C1	1.32	11	O2	Cu1	N2	107.6
12	O2	C6	1.198	12	O2	Cu1	O2	180
13	O3	C6	1.312	13	Cl1	Cu1	N2	89.6
14	O3	C7	1.46	14	Cl1	Cu1	O2	93.9
15	C2	C3	1.49	15	N2	Cu1	O2	72.4
16	C2	C4	1.362	16	N2	N1	C1	119.2
17	C4	C5	1.387	17	N2	N1	C2	111
18	C5	C6	1.467	18	C1	N1	C2	129.6
19	C7	C8	1.41	19	Cu1	N2	N1	131.2
20	N1	N2	1.344	20	Cu1	N2	C5	122.8

$C_{16}H_{24}Cl_2CuN_4O_6$ molecular formula, calc.: C, 38.22; H, 4.81, and N, 11.18. Found to be C, 37.88; H, 4.76, and N, 11.02. MS (*m/z*) calc. = 502.8 M^+ (Exp. = 501.4 M—H^+).

The qualitative composition and purity of the desired complex was confirmed by EDX analysis as in Fig. 1. The presence of Cu atoms was confirmed by energy sharp signals at 9.1, 8.2, and 1.2 keV and the Cl signal was cited to 2.4 keV position, meanwhile, the C, O, and N and atoms signals were cited to 0.4, 0.5 and 0.7 keV respectively, as seen in Fig. 6. The non-attendance of any other uncited peaks reflected a high degree of complex purity.

3.2. XRD investigation

The 3D-structure of the complex is depicted in Fig. 2a. Chosen specified set of geometrical parameters is listed in Table 2. The complex crystallized in the $P2_1/c$ space group with the monoclinic system and the copper(II) ion is located on a center of symmetry. The ester-substituted pyrazole acts as a bidentate chelating ligand, binding to the Cu(II) ion through the pyrazole nitrogen and the carbonyl oxygen atoms belong to carboxylate group. The Cu(II) coordination sphere $[CuN_2O_2Cl_2]$ includes, in addition to two center of symmetry related chelating ester-substituted pyrazole ligands, two *trans*-chloride ions. The geometry around the metal ion is distorted octahedral with a d^9 Jahn-Teller elongation along O—Cu—O axis (Cu—O: 2.565(4) Å) (Fig. 2b). The Cu-N and Cu-Cl bond lengths are 1.987(4) Å and 2.283

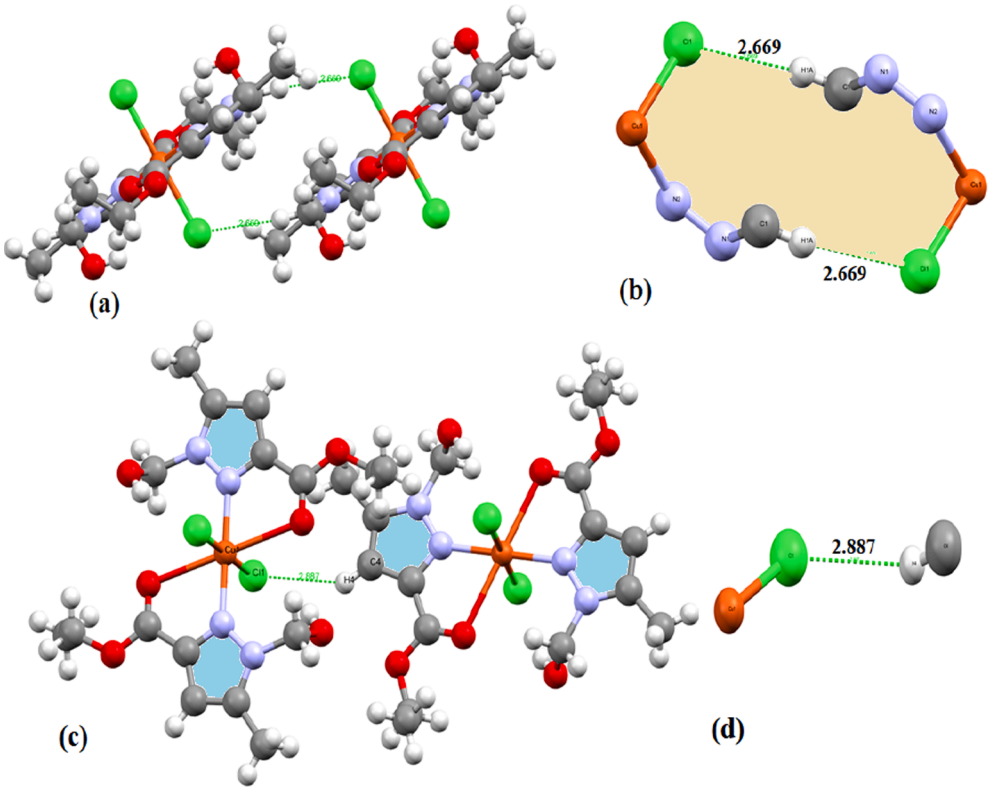

Fig.3. Total interactions types in the crystal lattice.

(2) Å respectively. The *cis*-angles are in the range 72.4(2)°–107.6(2)°. These geometrical data are similar to those reported for related compounds [26]. Intramolecular classical hydrogen bonding interactions (OH…Cl) and non-classical (CH…O) take place between the free pendant ligand hydroxyl group and the chloride ligand as well as between the N-methylene group and the carbonyl oxygen atom respectively. The complex molecules pack along the a-axis to form chains stabilized by intermolecular hydrogen bonding interactions of the type (CH…Cl) involving the N-methylene group. The molecular chains pack to form layers interconnected by a complex hydrogen-bonding network (Fig. 2c).

The interactions in the crystal lattice have been displayed as seen in Fig. 3a. Two types of C—H…..Cl-Cu H-bonds have been detected only, no OH….Cl, C—H•••N, π-π stacking C—H…π interactions were found. Two supramolecular synthons of like $R^2_2(12)$ *via* two similar OCH—H…. Cl-Cu H-bonds with 2.669 Å were recorded as seen in Fig. 3a and b. Four 1D supramolecular H-bonds like C_{ring}H….Cl-Cu with 2.887 Å were recorded as seen in Fig. 3c and d.

3.3. HSA and 2D-FP investigation

To understand the interactions modes on the surface of the molecule and its surrounding [27–33], HSA calculation was performed in 0.775–1.884 a. u. range and by using the cif file as seen observed in Fig. 4. The d_{norm} normalized surface mapped (Fig. 4a and b) and shape index (Fig. 4c) illustrated the presence of 8 red spots (4big + 4small) in the crystal surface of the molecule which played vital roles in stabilizing the lattice via two types of C—H….Cl-Cu Hydrogen bonds only. The four big spots were attributed to C_{Me}—H…..Cl (Fig. 4a–c) short H-bonds which were consistent with the two $R^2_2(12)$ supramolecular synthons formation. The other four small spots are due to C_{ring}—H….Cl that matched with 1D supramolecular long H-bonds formation. Moreover, the shape index showed a vastly different degree of electrons-based distribution among of the functional groups close to the outer surface of the compound, where the groups rich in electrons appeared with a red color, while the poor groups were displayed in the blue variant as seen in Fig. 4c. Accordingly, it is clear that the results of HSA are compatible with the XRD-packing result.

The 2D-FP plots were presented in Fig. 4d were considering outside to inside atoms as the closest-neighboring molecular contributions. The atom…atom contact ratios are resolved as H…H (70.6%), the larger contribution part and H…..Cu (0.0%) accounted for the lowest contribution interactions. The other atom…atom inter-molecular forces illustrated as [H…H > H…Cl > H…O > H…C > H…Cu] order.

3.4. ft-ir

The prepared complex and its free NNOH ligand IR spectra were illustrated in Fig. 5. A Couple of functional groups like O—H, aromatic and aliphatic C—H, C═N, C═O, N-N, and Cu—O, stretching-vibrations was recorded to their positions (see experimental part).

The occurrence of the coordination reaction was established by the significant deviation of the carbonyl group stretching frequency from 1790 to 1750 cm^{-1} consistent with the formation of Cu—O = coordination bonds, and the occurrence of two new signals at 460 and 445 cm^{-1} assigned to the formation of Cu—O and Cu—N bonds, respectively [27–29]. Moreover, no significant change in O-H vibrations was observed before and after coordination reaction, supporting the fact of the uncoordinated OH group in the complex.

3.5. Electronic transfer

The electronic absorption of the free NNOH ligand was compared to its complex in MeOH solvent as illustrated in Fig. 6. In both NNOH and its complex spectra, the diagram showed a strong series of UV peaks at the same λ_{max} with 280 nm that is attributed to the ligand $\pi \rightarrow \pi^*$ e-transition (Fig. 6a). The complex spectrum showed a very wide band in the visible green region at λ_{max} = 670 nm assigned to d-d transitions in

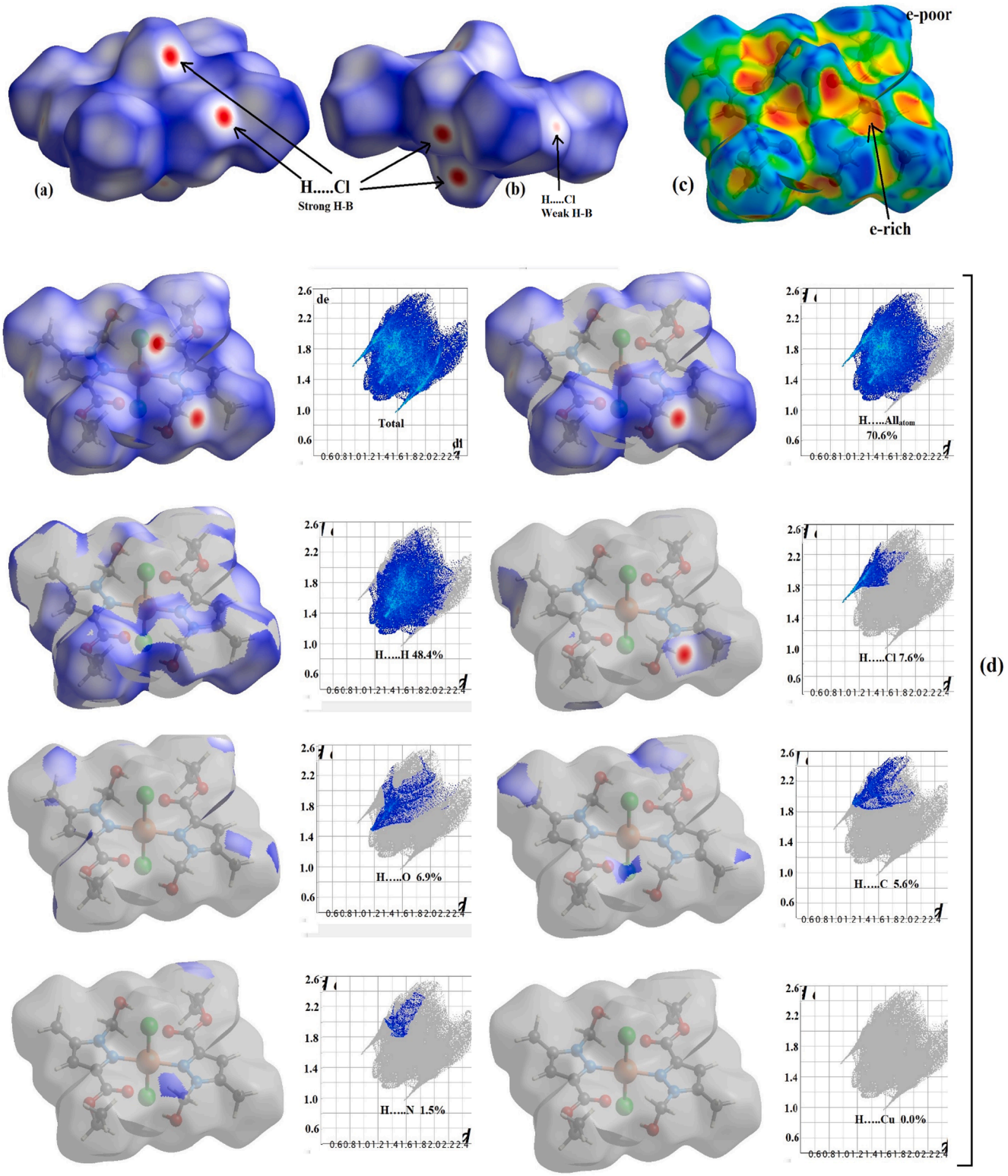

Fig.4. HSA mapped: (a–c) d_{norm}, (d) shape index and (d) outside/inside 2D-FP plots.

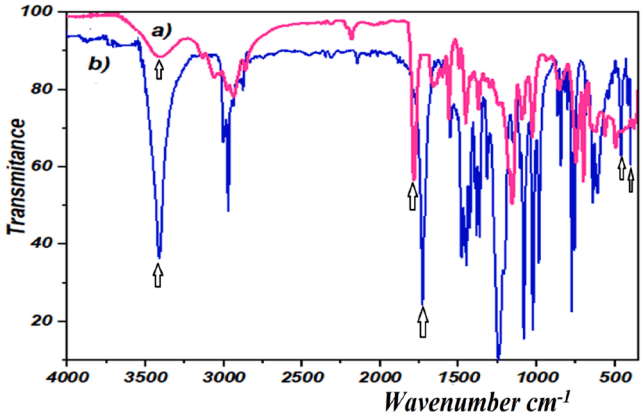

Fig.5. FT-IR of: (a) NNOH free ligand, and (b) the desired complex.

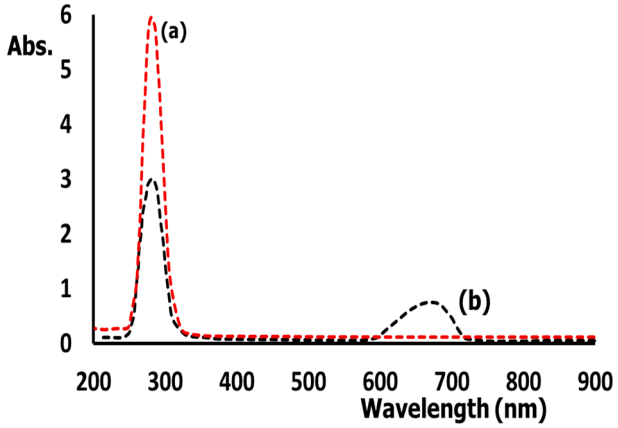

Fig.6. RT UV–Vis spectra, (a) free NNOH ligand, and (b) the complex in MeOH solvent.

the octahedral Cu(II) center (Fig. 6b). The peak profile is consistent with Jahn- Teller distortion in the complex, as determined in the solid state from single crystal X-ray data.

3.6. Antifungal and antibacterial activities

The results of antifungal activities of the desired complex are illustrated in Fig. 7a. In general, the complex displayed excellent activities against *Aspergillus flavus, Penicillium marneffei, Candida albicans and Cryptococcus neoformans* fungi sereis. For example, the complex showed an excellent range of activity against, *Penicillium marneffei* (12 mm) and *Cryptococcus neoformans* (25 mm) with higher or equal activities compared to the Ketoconazole reference antifungal well-known medicine see Fig. 7a. In the case of *Aspergillus flavus* (15 mm) and *Candida albicans* (18 mm), the complex activity is comparable to Ketoconazole activities; therefore, the complex can be classified as an excellent antifungal agent.

The synthesized complex was subjected to an antibacterial studies against two strains of Gram-negative bacteria [Proteus vulgaris and Escherichia coli] and two strains of Gram-positive bacteria [Staphylococcus aureus and Bacillus subtilis] by the diffusion agar technique. The screening results of antibacterial are presented in Fig. 7b. The complex showed very strong activity against Bacillus subtilis (22 mm) and Proteus vulgaris (20 mm), in all cases, the complex did not outperform the Gentamycin antibiotic reference. Furthermore, the complex reflected a weak behavior against Staphylococcus aureus one (14) and a very weak a significantly low level of activity against Escherichia coli (13 mm). The complex displayed higher antifungal efficacy against all the fungi used in comparison to antibacterial activities.

4. Conclusion

The *trans*-$Cl_2Cu(NNOH)_2$ complex based on ethyl-1-(hydroxymethyl)-5-methy-3-carboxylatel pyrazole polydentate ligand has been prepared under microwave mode of irradiation *via* one-pot process. The 3D-structure of the complex together with internal interactions synthons was identified *via* single-crystal XRD-analysis. A slightly distorted octahedral geometry around Cu(II) center has been determined, in addition the EDX, UV–Vis, FT-IR, EDS, and CHN-EA analysis supported the complex molecular composition. The HSA and 2D-FP stimulation confirmed the formation of several O—H…H and C—H…Cl H-bonds collected experimentally by the XRD-packing result. The complex showed exhibited excellent range of antifungal activities against four types of fungi and very good level of activities against both gram negative and positive bacterial strains.

Declaration of Competing Interest

The authors declare that they have no known competing financial interests or personal relationships that could have appeared to influence the work reported in this paper.

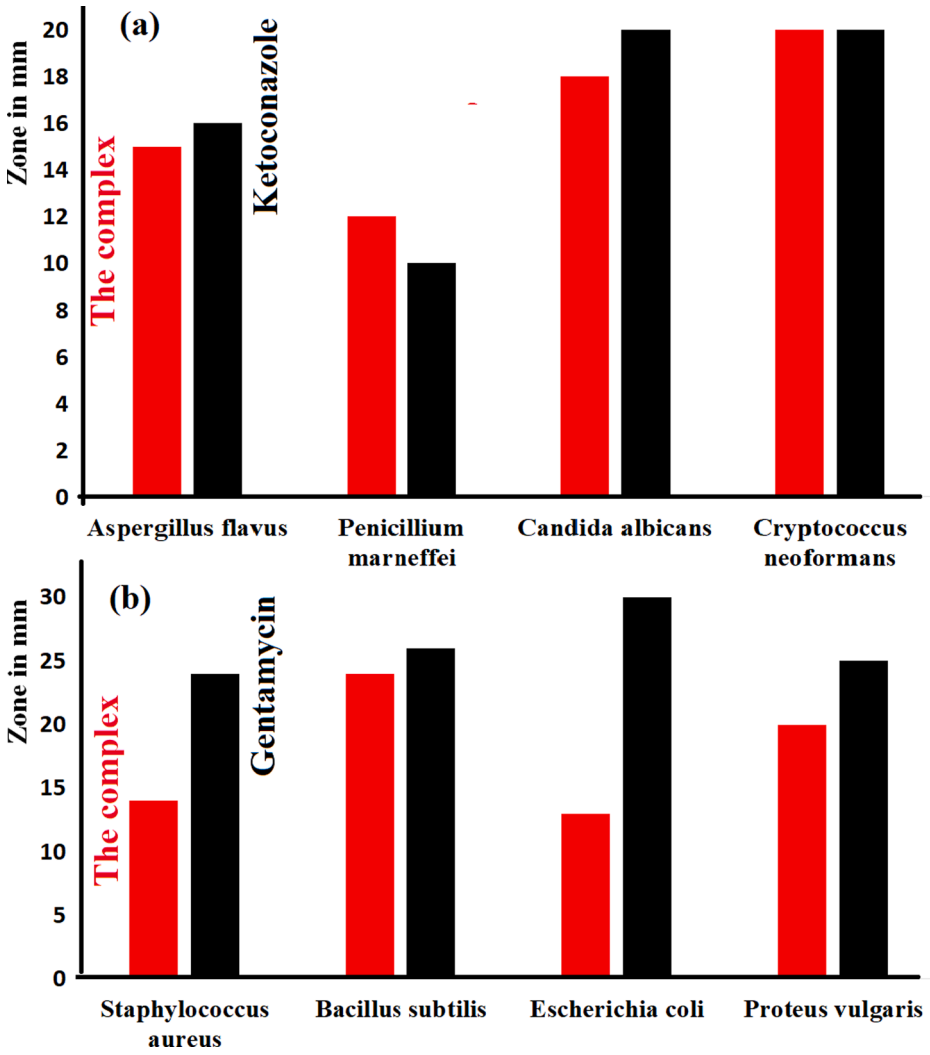

Fig.7. Antimicrobial activities of the desired complex (a) Antifungal and, (b) antibacterial.

References

[1] G. Nitulescu, C. Draghici, T. Olaru, Int. J. mol. Sci. 14 (2013) 21805.
[2] G. Nitulescu, C. Draghici, V. Missir AV., Eur J Med Chem. 45 (2010) 4914.
[3] A. Titi M. Messali A. Alqurashy R. Touzani T. Shiga H. Oshio T. Hadda J. Mol. Struc. 1205 2020 127625.
[4] T.D. Penning, J.J. Talley, S.R. Bertenshaw, J.S. Carter, P.W. Collins, S. Docter, M. J. Graneto, L.F. Lee, J.W. Malecha, J.M. Miyashiro, R.S. Rogers, D.J. Rogier, S. S. Yu, G.D. Anderson, E.G. Burton, J.N. Cogburn, S.A. Gregory, C.M. Koboldt, W. E. Perkins, K. Seibert, A.W. Veenhuizen, Y.Y. Zhang, P.C. Isakson, J. Med. Chem. 40 (1997) 1347.
[5] J. Regan, S. Breitfelder, P. Cirillo, T. Gilmore, A.G. Graham, E. Hickey, B. Klaus, J. Madwed, M. Moriak, N. Moss, C. Pargellis, S. Pav, A. Proto, A. Swinamer, L. Tong, C. Torcellini, J. Med. Chem. 45 (2002) 2994.
[6] M.J. Genin, C. Biles, B.J. Keiser, S.M. Poppe, S.M. Swaney, W.G. Tarpley, Y. Yagi, D.L. Romero, J. Med. Chem. 43 (2000) 1034.
[7] P. Lei, X. Zhang, Y. Xu, G. Xu, X. Liu, X. Yang, X. Zhang, Y. Ling, Chem. Cent. J. 10 (2016) 40.
[8] F. Marchetti, C. Pettinari, R. Pettinari, Coord. Chem. Rev. 249 (2005) 2909.
[9] R. Bose, D.S.R. Murty, G. Chakrapani, J. Radioanal. Nucl. Chem. 265 (2005) 115.
[10] J.W. Roebuck, J.R. Turkington, D.M. Rogers, P.J. Bailey, V. Griffin, A. J. Fischmann, G.S. Nichol, M. Pelser, S. Parsons, P.A. Tasker, Dalton Trans. 45 (2016) 3734.
[11] T. Ito, C. Goto, K. Noguchi, Anal. Chim. Acta 443 (2001) 41.
[12] J. Guo, D. Jia, L. Liu, H. Yuan, F. Li, J. Mater. Chem. 21 (2011) 3210.
[13] C.E. Weston, R.D. Richardson, P.R. Haycock, A.J.P. White, M.J. Fuchter, J. Am. Chem. Soc. 136 (2014) 11878.
[14] J. Guo, L. Liu, D. Jia, M. Guo, Y. Zhang, X. Song, New J. Chem. 39 (2015) 3059.
[15] J. Xu, K. Du, J. Shen, Ch. Shen, K. Chai, P. Zhang, ChemCatChem. 10 (2018) 3675.
[16] H. Yi, H. Chen, C. Bian, Z. Tang, A.K. Singh, X. Qi, X. Yue, Y. Lan, J.-F. Lee, A. Lei, Chem. Commun. 53 (2017) 6736.
[17] A.I. Uraev, K.A. Lyssenko, V.G. Vlasenko, Y.V. Zubavichus, M.P. Bubnov, N. I. Makarova, A.S. Burlov, Polyhedron 146 (2018) 1.
[18] K. Singh, Y. Kumar, P. Puri, M. Kumar, C. Sharma, Eur. J. Med. Chem. 52 (2012) 313.
[19] D.A. Garnovskii, S.I. Levchenkov, G.G. Aleksandrov, N.I. Makarova, V.G. Vlasenko, V.Y. Zubavichus, A.A. Burlov, J. Coord. Chem 42 (2016) 755.
[20] A. Aljuhani, M.R. Aouad, N. Rezki, O.A. Aljaldy, S.A. Al-Sodies, M. Messali, I. Ali, J. Mol. Liq. 285 (2019) 790.
[21] S.K. Wolff, D.J. Grimwood, J.J. McKinnon, D. Jayatilaka, M.A. Spackman, Crystal explorer 2.1, University of Western Australia, Perth, 2007.
[22] Bruker, (2017). Apex3 v2017.3-0, SAINT V8.38A, Bruker AXS Inc.: Madison (WI), USA, 2013/2014.
[23] L. Krause, R. Herbst-Irmer, G.M. Sheldrick, D. Stalke, J. Appl. Crystallogr. 48 (2015) 3.
[24] G.M. Sheldrick, Acta cryst. A 71 (2015) 3.
[25] J.D. Silversides, C.C. Allan, S, J. Arch. Dal Trans. 34 (2007) 971.
[26] S. Shin, S. Nayab, H. Lee, Poly 141 (2018) 309.
[27] A. Titi, T. Shiga, H. Oshio, R. Touzani, B. Hammouti, M. Mouslim, I. Warad, J. Mol. Stru. 1199 (2020), 126995.
[28] A. Titi, I. Warad, M. Tillard, R. Touzani, M. Messali, M. El Kodadi, A. Zarrouk, J. Mol. Stru. 1217 (2020) 128422.
[29] A. Titi, H. Oshio, R. Touzani, M. Mouslim, A. Zarrouk, B. Hammouti, I. Warad, J. Clust. Sci. 12 (2020) 1.
[30] M.R. Aouad, M. Messali, N. Rezki, N. Al-Zaqri, I. Warad, J. Mol. Liq. 264 (2018) 621.
[31] I. Warad, H. Suboh, N. Al-Zaqri, A. Alsalme, F.A. Alharthi, M.M. Aljohanie, A. Zarrouk, RSC Adv. 10 (2020) 21806.
[32] C. Chiter, A. Bouchama, T.N. Mouas, H. Allal, M. Yahiaoui, I. Warad, A. Zarrouk, Amel Djedouani. J. Mol. Stru. 1217 (2020) 128376.
[33] M.K. Hema, I. Warad, C.S. Karthik, A. Zarrouk, K. Kumara, K.J. Pampa, P. Mallu, N. K. Lokanath, J. Mol. Stru. 1210 (2020) 128000.

Ismail Warad